

Detecting Higher Berry Phase via Boundary Scattering

Chih-Yu Lo¹ and Xueda Wen¹

¹*School of Physics, Georgia Institute of Technology, Atlanta, GA 30332, USA*

Higher Berry phase has recently been proposed to study the topology of the space of gapped many-body quantum systems. In this work, we develop a boundary-scattering approach to detect higher Berry phases in one-dimensional gapped free-fermion systems. By coupling a gapless lead to the gapped system, we demonstrate that the higher Berry invariant can be obtained by studying the higher winding number of the boundary reflection matrix. The resulting topological invariant is robust against perturbations such as disorder. Our approach establishes a connection between higher Berry invariants and transport properties, thereby providing a potentially experimentally accessible probe of parametrized topological phases.

I. INTRODUCTION

Higher Berry phase, the many-body generalization of Berry phase of parameterized quantum systems, was proposed to study the space of gapped many-body systems and, more broadly, the topological properties of parametrized gapped phases [1–48]. This interest has been largely driven by Kitaev’s conjecture [1–3], which proposes that invertible phases of matter are classified by generalized cohomology theories. To probe the topology of the space of gapped many-body systems, Kapustin and Spodyneiko proposed the concept of higher Berry curvatures for general gapped many-body lattice systems [6, 7]. This concept was subsequently developed in a systematic way within the framework of operator algebras, covering both symmetric and symmetry-breaking settings [8]. The flux of higher Berry curvature through a surface in the parameter space defines the higher Berry phase; when the surface is closed, this quantity becomes a topological invariant, often referred to as the higher Berry invariant.

Physically, a nonzero higher Berry invariant is associated with a topological pump in a parametrized gapped system. More generally, the higher Berry curvature in d -dimensional systems can be interpreted as describing a flow of higher Berry curvature in $(d - 1)$ -dimensional systems [15]. In one dimension, this picture reduces to a flow of ordinary Berry curvature in real space, giving rise to the intriguing phenomenon of Chern number pumping [15, 24, 28, 34].

Recent developments have clarified the wavefunction-level meaning of higher Berry invariants. A nonzero higher-Berry invariant implies that the family of ground states carries a gerbe structure, generalizing the line bundle familiar from ordinary Berry phases. When this gerbe is nontrivial, there is an obstruction to representing the ground states by a globally continuous matrix-product-state tensor over parameter space [23, 24].

Subsequent works have shown that higher Berry curvatures can be constructed directly from MPS representations, both in one dimension [28, 30] and in higher dimensions [29, 31], providing a natural extension of the original Hamiltonian-based construction [6].

More recently, higher Berry phases have been extended to the study of spaces of conformal boundary conditions,

or equivalently, conformal boundary states [36, 37]. One can define higher Berry connections and curvatures on the space of conformal boundary conditions using correlation functions of boundary-condition-changing operators [36]. Physically, parametrized conformal boundary conditions can induce a flow of Berry curvature and, correspondingly, a Chern-number pump in boundary conformal field theories [37]. This phenomenon closely mirrors the Berry-curvature flow in one-dimensional gapped systems [15, 24, 28, 34].

Higher Berry invariants also constrain phase diagrams [9]. If the parameter space X lies entirely within a gapped region, the family of Hamiltonians defined over X captures global topological information about that region. From this viewpoint, conventional gapped phases correspond to connected components of the space of Hamiltonians, while parametrized families probe more refined topological structures. This perspective has stimulated recent interest in parametrized systems and in the structure of critical points in phase diagrams [9, 38–42, 47–51].

Despite these conceptual advances, an important practical question remains open: How can higher Berry invariants be detected experimentally? More specifically, can information about these invariants be extracted solely from boundary probes, without accessing the bulk wavefunction or Hamiltonian directly?

A. Motivations and Setup

Our motivations are twofold.

First, from a conceptual perspective, it has recently been shown that coupling a conformal field theory to a parametrized gapped system drives the interface toward parametrized conformal boundary conditions under renormalization [36, 37]. In this picture, the higher Berry phase of the bulk manifests as a Berry-curvature flow in the boundary CFT [37]. Since this flow is determined by how the boundary reflects gapless modes, it is natural to ask whether the higher Berry invariant can be extracted directly from the boundary data itself, without analyzing the induced spectral flow.

Second, from an experimental standpoint, directly

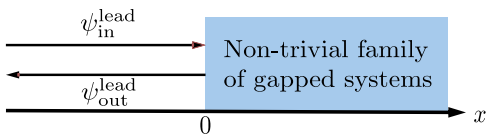


FIG. 1. Schematic illustration of detecting the topological invariant of a parametrized family of gapped systems via boundary scattering. In the limit where the gapped system is infinitely long, an incoming wavefunction $\psi_{\text{in}}^{\text{lead}}$ from the left lead is completely reflected into an outgoing wavefunction $\psi_{\text{out}}^{\text{lead}}$. The resulting reflection matrix $R(\lambda)$ as defined in (1.1) depends on the gapped-system parameters λ . As these parameters are varied, the evolution of R in parameter space defines a quantized topological winding number.

measuring bulk higher Berry invariants is typically challenging. If the same information is encoded in boundary scattering processes, then boundary probes may provide a practical route to detecting higher Berry phases.

To address these questions, we consider a one-dimensional parametrized family of gapped systems coupled to a gapless lead, as illustrated in Fig. 1. The lead is in the region $(-\infty, 0)$, while the parametrized gapped system resides in $(0, +\infty)$, with the interface located at $x = 0$. Our goal is to show that the higher Berry invariant of the bulk family can be extracted entirely from the reflection matrix at this interface.

Throughout this work, we focus on free-fermion insulators with a global $U(1)$ charge symmetry. Although the presence of $U(1)$ symmetry is not strictly necessary for realizing higher Berry phases, it allows for a particularly transparent formulation in terms of charge transport and scattering. This perspective also facilitates experimental access, as the relevant quantities can, in principle, be probed through interference and electrical conductivity measurements [52].

When the energy of an incoming electron from the lead lies within the bulk gap of the insulator, transmission is suppressed and the electron is completely reflected at the interface (See Fig.1)

$$\psi_{\text{out}}^{\text{lead}}(0) = R(\lambda) \psi_{\text{in}}^{\text{lead}}(0). \quad (1.1)$$

That is, the total reflection is described by a unitary reflection matrix R , which depends smoothly on the parameters λ characterizing the Hamiltonian of the gapped system.

We assume that the parameter space X of the gapped Hamiltonians forms a smooth manifold. The reflection matrix R then defines a smooth map

$$R: X \rightarrow U(N), \quad (1.2)$$

where N in the unitary matrix $U(N)$ denotes the number of propagating channels in the lead. For example, for a single spinless lead with one right- and one left-moving mode, we have $N = 1$.

It is well known that, in the presence of global $U(1)$ symmetry, tuning the parameters along a closed loop in

the parameter space can realize a nontrivial Thouless charge pump [53]. The associated topological invariant can be expressed purely in terms of the reflection matrix as [54–58]

$$\nu_1(R) = \frac{1}{2\pi i} \int_{X=S^1} \text{Tr}(R^\dagger dR) \in \mathbb{Z}. \quad (1.3)$$

In this work, we propose that higher Berry invariants can be detected in a completely analogous manner. For a gapped system defined over a three-dimensional parameter space X , taken to be a closed manifold, we introduce the higher winding number, expressed in terms of the boundary reflection matrix, as

$$\nu_3(R) = \frac{1}{24\pi^2} \int_X \text{Tr}(R^\dagger dR)^3 \in \mathbb{Z}. \quad (1.4)$$

This expression is motivated by two key observations.

First, given a smooth map as defined in (1.2), with X a d -dimensional closed manifold, one can always define a d -dimensional winding number [59]. The integer in Eq. (1.4) is precisely the homotopy class of the map in (1.2).¹

Second, previous works [61–68] have demonstrated that, for free-fermion gapped Hamiltonians in general dimensions with fixed parameters, the complete bulk topological information is encoded in the boundary/surface scattering matrix. For instance, if one imposes translation invariance along the spatial directions parallel to the surface and interprets the parameter λ as the crystal momentum k in those directions, then (1.4) reduces to the boundary invariant associated with the second Chern number of four-dimensional topological insulators. In the present work, however, we treat λ as an external control parameter. The bulk-boundary correspondence (for boundary scattering) established in [61–68] can be naturally extended to such parametrized families of gapped free-fermion systems [67]. This extension leads to our boundary-scattering characterization of higher Berry phases in one-dimensional systems.

We study this boundary-scattering approach in both continuum field theories and lattice models. In particular, for lattice realizations we demonstrate that the topological invariant defined in (1.4) remains robust against perturbations such as disorder.

The remainder of this paper is organized as follows. In Sec. II, we begin with a field-theoretic analysis of the setup. We then turn to explicit lattice realizations in Sec. III, where we investigate both exactly solvable models and disordered models that are not analytically tractable. In Sec. IV, we conclude with a discussion of possible generalizations to parametrized gapped systems in higher spatial dimensions. Several appendices provide technical details, including explicit calculations of the reflection matrices for the lattice models.

¹ See also the recent work [60], which studies the quantization of ν_3 , even when X is replaced by a discrete approximation.

II. FIELD THEORY ANALYSIS

Before analyzing lattice realizations, it is useful to first understand how the formulas in (1.3) and (1.4) are implemented in field theory. To this end, we revisit the examples recently discussed in [9, 37].

A. Detect $U(1)$ Thouless pump

We consider the setup shown in Fig. 1, where the gapped system is described by a massive Dirac fermion with a global $U(1)$ symmetry, and the parameter space is $X = S^1$. The parametrized Hamiltonian takes the form

$$H_{\text{gap}} = \int_0^{+\infty} dx \Psi^\dagger(x) (-i\sigma_3 \partial_x + m_0 \sigma_1 + m_1 \sigma_2) \Psi(x), \quad (2.1)$$

where $\Psi(x) = (\psi_R(x), \psi_L(x))^T$ is the Dirac fermion operator with right- and left-moving components, and σ_i are Pauli matrices acting in the chiral basis. The mass parameters (m_0, m_1) are chosen to lie on the circle $X = S^1$, which we parametrize as

$$m_1 + im_0 = m e^{i\alpha}, \quad \alpha \in [0, 2\pi], \quad (2.2)$$

with fixed amplitude $m > 0$. As α is adiabatically varied from 0 to 2π , the system realizes a quantized charge pump along the one-dimensional bulk, i.e., the Thouless pump [53]. For the lead in Fig. 1, we take a gapless Dirac fermion of the same form as in (2.1), but with the mass term set to zero. Following the method in [37], one finds that the boundary reflection condition at $x = 0$ is

$$\psi_{\text{out}}(x=0) = e^{-i\alpha} \psi_{\text{in}}(x=0), \quad \alpha \in [0, 2\pi]. \quad (2.3)$$

Thus, the reflection matrix is simply

$$R = e^{-i\alpha}. \quad (2.4)$$

As α winds once around S^1 , the reflection phase acquires a nontrivial winding, yielding the quantized invariant $\nu_1 = -1$ according to (1.3). This boundary winding number faithfully captures the bulk topological response, i.e., the quantized charge pumping in the gapped system.

B. Detect higher Berry invariant

Now let us consider a gapped system with a nontrivial higher Berry phase. The parametrized gapped Hamiltonians we will consider in Fig.1 are [9, 37]

$$H_{\text{gap}} = \int_0^{+\infty} dx \left[-i(\mathbb{I} \otimes \sigma_3) \partial_x + m_0(\mathbb{I} \otimes \sigma_1) + \sum_{j=1}^3 m_j (\sigma_j \otimes \sigma_2) \right], \quad (2.5)$$

where the parameter space is taken to be $X = S^3$, subject to the constraint $\sum_{\mu=0}^3 m_\mu^2 = 1$.

Physically, as the parameters are varied over $X = S^3$, the system exhibits a flow of the conventional two-form Berry curvature, resulting in a quantized Chern-number pump along the one-dimensional system [15, 28, 37].

For the lead in Fig. 1, we take the same Hamiltonian (2.5) but set the mass terms to zero. Solving the corresponding scattering problem yields the reflection matrix [37]²

$$R = m_0 \mathbb{I} + i \sum_{k=1}^3 m_k \sigma_k \in SU(2). \quad (2.6)$$

To parametrize S^3 , we introduce

$$\begin{aligned} m_0 &= \cos \alpha, & m_1 &= \sin \alpha \cos \theta, \\ m_2 &= \sin \alpha \sin \theta \cos \phi, & m_3 &= \sin \alpha \sin \theta \sin \phi, \end{aligned} \quad (2.7)$$

with $\alpha, \theta \in [0, \pi]$ and $\phi \in [0, 2\pi]$. Substituting R with this parametrization into (1.4), we find that the higher Berry invariant associated with the reflection matrix is $\nu_3[R] = -1$. This integer quantifies the Chern-number pump along the one-dimensional gapped system [15, 28, 37].

In the next section, we construct an explicit lattice realization of this field theory and compute the same topological invariant from the lattice scattering problem.

III. DETECT HIGHER BERRY PHASE VIA BOUNDARY SCATTERING: IN LATTICE MODELS

In this section, we implement the boundary-scattering approach to detect higher Berry phases in lattice models. We analyze both exactly solvable models and models that are not analytically tractable. While our primary focus is on systems exhibiting higher Berry phases, we also include, in Appendix B, a complementary discussion on detecting the conventional $U(1)$ Thouless charge pump using the same approach.

A. Setup and Method

Let us first give an overview of our setup and method. More details can be found in Appendix A.

We consider a family of one-dimensional, gapped, short-range-entangled free-fermion systems described by

² Note that, from the perspective of boundary conformal field theory (BCFT), the parametrized reflection matrices can be interpreted as twisted boundary conditions. Adiabatically changing this twisted boundary condition will induce a multi-parameter spectral flow in the BCFT [37]. In the present work, however, we extract the topological information directly from the reflection matrices, without analyzing the spectral flow.

the Hamiltonian

$$H_{\text{gap}} = \sum_{i=0}^{2L-1} (-1)^i \psi_i^\dagger \vec{m} \cdot \vec{\sigma} \psi_i + \sum_{i=0}^{L-1} f_+(m_0) (\psi_{2i+1}^\dagger \psi_{2i} + \text{h.c.}) + \sum_{i=1}^L f_-(m_0) (\psi_{2i-1}^\dagger \psi_{2i} + \text{h.c.}), \quad (3.1)$$

where $\psi_i = (\psi_{i,\uparrow}, \psi_{i,\downarrow})$ contain two complex fermions, $\vec{m} = (m_1, m_2, m_3)^T$ are the mass parameters that are real, and $\vec{\sigma} = (\sigma_1, \sigma_2, \sigma_3)^T$ are the Pauli matrices. The functions $f_+(m_0)$ and $f_-(m_0)$ represent tunable hopping amplitudes that depend on an additional parameter m_0 . The four parameters (m_0, \vec{m}) define our parameter space $X = S^3$, subject to the constraint

$$|\vec{m}|^2 + m_0^2 = 1. \quad (3.2)$$

Note that the Hamiltonian in (3.1) is fully gapped when defined on an infinite chain. However, in the presence of an open boundary, gapless boundary modes may emerge for certain regions of the parameter space. For the lead shown in Fig. 1, we consider a gapless free-fermion chain that is coupled to the gapped system. The total Hamiltonian then takes the form

$$H = \sum_{i<0} \frac{v_0}{2} (\psi_i^\dagger \psi_{i+1} + \text{h.c.}) + H_{\text{gap}}, \quad (3.3)$$

where $\psi_i = (\psi_{i,\uparrow}, \psi_{i,\downarrow})$, and v_0 denotes the group velocity in the lead. We choose the coupling between the lead and the sample to be identical to the hopping amplitude within the lead itself. Throughout this work, we choose the Fermi energy at zero energy, which lies inside the bulk gap of H_{gap} .

For $j \leq 0$ in the lead, we assume the scattering ansatz

$$\psi_j = (e^{ikj} \mathbb{I} + e^{-ikj} R) A_0, \quad (3.4)$$

where R is the reflection matrix and A_0 is an arbitrary vector that describe the spin components of the incoming wave. This allows us to package the semi-infinite lead into a self energy $\Sigma_0 = \frac{1}{2} v_0 e^{ik}$ as well as an effective source $q_0 = -i v_0 \sin k A_0$ both localized at site 0 (See Appendix A). Therefore, the wave function ψ_j for this scattering problem can be solved by

$$\psi_0 = G_{00}(\omega) q_0, \quad (3.5)$$

where $G(\omega) = (\omega I - H_{\text{gap}} - \Sigma_0)^{-1}$ is the Green's function for the effective Hamiltonian with self energy and effective source, which is obtained by the continued fraction method on lattice. By wave function matching, we can then solve for the reflection matrix

$$R(\omega) = -\mathbb{I} - i v_0 \sin k G_{00}(\omega). \quad (3.6)$$

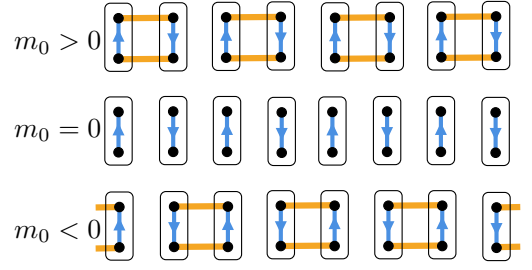


FIG. 2. Exactly solvable free-fermion lattice models that exhibit a nontrivial higher Berry phase with parameter space $X = S^3$. Each super-site (black box) contains two sites, and the orange lines correspond to the hopping characterized by m_0 . Each blue line corresponds to a hopping characterized by $\vec{m} = (m_1, m_2, m_3)^T$. These parameters satisfy the constraint in (3.2).

B. Exactly solvable model

We first consider an exactly solvable model inspired by the suspension construction proposed in [15].

As illustrated in Fig. 2, we take the Hamiltonian in Eq. (3.1) and specify the functions

$$f_+ = \begin{cases} m_0, & 0 \leq m_0 \leq 1, \\ 0, & \text{otherwise,} \end{cases} \quad (3.7)$$

and

$$f_- = \begin{cases} -m_0, & -1 \leq m_0 \leq 0, \\ 0, & \text{otherwise.} \end{cases} \quad (3.8)$$

The physical idea underlying this construction is the following. When $m_0 = 0$, the one-dimensional system reduces to a collection of decoupled zero-dimensional subsystems. The Hamiltonian for the i -th super-site (see Fig.2) takes the form

$$H_{0d}^i = (-1)^i \psi_i^\dagger \vec{m} \cdot \vec{\sigma} \psi_i. \quad (3.9)$$

For each super-site, the ground state carries a Chern number ± 1 over the parameter space S^2 defined by $|\vec{m}|^2 = 1$, with the sign alternating between neighboring super-sites due to the factor $(-1)^i$. Turning on m_0 couples adjacent super-sites in a dimerized pattern. For $m_0 < 0$, the coupling occurs between the $(2i - 1)$ -th and $2i$ -th super-sites. In contrast, for $m_0 > 0$, the coupling is shifted to connect the $2i$ -th and $(2i + 1)$ -th super-sites. This switching mechanism is essential for realizing the suspended topological structure of the model and leads to a quantized Chern-number pump, as analyzed in detail in [15].

Due to the dimerized structure described above, the analysis of the reflection matrix reduces to a minimal two-super-site problem. It is therefore sufficient to consider the following effective Hamiltonian for the gapped system. For $m_0 > 0$, we take

$$H_{\text{dimer}} = \psi_0^\dagger \vec{m} \cdot \vec{\sigma} \psi_0 - \psi_1^\dagger \vec{m} \cdot \vec{\sigma} \psi_1 + m_0 (\psi_1^\dagger \psi_0 + \psi_0^\dagger \psi_1), \quad (3.10)$$

while for $m_0 \leq 0$, the system reduces to a single decoupled super-site,

$$H_{\text{dimer}} = \psi_0^\dagger (\vec{m} \cdot \vec{\sigma}) \psi_0. \quad (3.11)$$

In this simplified setting, the local Green's function G_{00} can be computed analytically. One finds

$$G_{00} = \begin{cases} \left(-\vec{m} \cdot \vec{\sigma} - \frac{iv_0}{2} + m_0^2 (\vec{m} \cdot \vec{\sigma})^{-1} \right)^{-1}, & m_0 > 0 \\ \left(-\vec{m} \cdot \vec{\sigma} - \frac{iv_0}{2} \right)^{-1}, & m_0 \leq 0 \end{cases} \quad (3.12)$$

Substituting these expressions into (3.6), we obtain the corresponding reflection matrix R . For the parametrization given in (2.7), the three-dimensional winding number reads

$$\nu_3(R) = \frac{1}{4\pi^2} \int_X [\text{Tr}(R^\dagger dR)^{\wedge 3}]_{\alpha\theta\phi} d\alpha \wedge d\theta \wedge d\phi, \quad (3.13)$$

where

$$\text{Tr}(R^\dagger dR)^{\wedge 3} = \begin{cases} \frac{-1024 \cos \alpha \sin^2 \alpha \sin \theta}{(-9 + \cos 2\alpha)^3}, & m_0 > 0, \\ \frac{-128 \cos \alpha \sin^2 \alpha \sin \theta}{(-3 + 2 \cos 2\alpha)^3}, & m_0 \leq 0. \end{cases} \quad (3.14)$$

The integral can then be carried out analytically, leading to the quantized higher Berry invariant

$$\nu_3(R) = -1. \quad (3.15)$$

This invariant characterizes the quantized Chern number pump in the one dimensional gapped system [15, 28, 37].

C. General free fermion chain

We now turn to a more general situation by introducing a uniform hopping term, so that the system can no longer be viewed as a collection of decoupled dimers. Concretely, we modify the functions in Eqs. (3.7) and (3.8) according to

$$f'_\pm = \frac{v_1}{2} + f_\pm, \quad (3.16) \quad \text{with}$$

$$r = \begin{cases} \begin{cases} -\frac{m^2 + m_0 v_1 + m \sqrt{|\vec{m}|^2 + (m_0 + v_1)^2} - i|\vec{m}|v_0}{m^2 + m_0 v_1 + m \sqrt{|\vec{m}|^2 + (m_0 + v_1)^2} + i|\vec{m}|v_0}, & m_0 > 0, \\ -\frac{-m_0^2 + |\vec{m}|^2 + m_0 v_1 + m \sqrt{|\vec{m}|^2 + (m_0 - v_1)^2} - i|\vec{m}|v_0}{-m_0^2 + |\vec{m}|^2 + m_0 v_1 + m \sqrt{|\vec{m}|^2 + (m_0 - v_1)^2} + i|\vec{m}|v_0}, & m_0 \leq 0. \end{cases} \end{cases} \quad (3.21)$$

where the parameter v_1 controls the strength of the additional uniform hopping. As a result, the system becomes fully connected, and the reflection matrix must be obtained by considering scattering from the entire chain rather than from an isolated dimer.

As shown in Appendix A, the Green's function at the super-site 0 for a chain $j \geq 0$ can be expressed as the Green's function at site 1 for the chain with $j \geq 1$ as follows:

$$G_{00}^{j \geq 0} = \left(-\vec{m} \cdot \vec{\sigma} - \frac{v_0}{2} e^{ik} - \left(\frac{v_1}{2} + m_0 \right)^2 G_{11}^{j \geq 1} \right)^{-1}. \quad (3.17)$$

Similarly, the Green's function for the chain with $j \geq 1$ can be written recursively in terms of that for the chain with $j \geq 2$. Iterating this procedure systematically shortens the chain and leads to a continued-fraction representation of the Green's function.

In the thermodynamic limit $L \rightarrow \infty$, the calculation simplifies considerably. The key observation is that the semi-infinite chain becomes self-similar: removing one unit cell (two super-sites in the present model) leaves the remaining chain invariant. For instance, one has $G_{11}^{j \geq 1} = G_{33}^{j \geq 3}$. As a result, $G^{j \geq 1}$ can be determined by solving the following self-consistent matrix equation:

$$(G_{11}^{j \geq 1})^{-1} = \vec{m} \cdot \vec{\sigma} - \left(\frac{v_1}{2} - m_0 \right)^2 \left(-\vec{m} \cdot \vec{\sigma} - \left(\frac{v_1}{2} + m_0 \right)^2 G_{11}^{j \geq 1} \right)^{-1}. \quad (3.18)$$

This self-consistent equation fully determines the Green's function and forms the basis for computing the reflection matrix of the infinite chain.

In our lattice model, we can diagonalize $G_{11}^{j \geq 1}$ by

$$U(\theta, \phi) = \begin{pmatrix} \cos \frac{\theta}{2} & -e^{i\phi} \sin \frac{\theta}{2} \\ e^{-i\phi} \sin \frac{\theta}{2} & \cos \frac{\theta}{2} \end{pmatrix}, \quad (3.19)$$

such that the matrix equation in (3.18) becomes two decoupled quadratic equations. We can write down the analytic form for the reflection matrix as

$$R = U^\dagger \begin{pmatrix} r & 0 \\ 0 & r^* \end{pmatrix} U, \quad (3.20)$$

Based on (1.4), (3.20), and (3.21), one finds that $\nu_3(R) = -1$, in agreement with the result (3.15) obtained in the

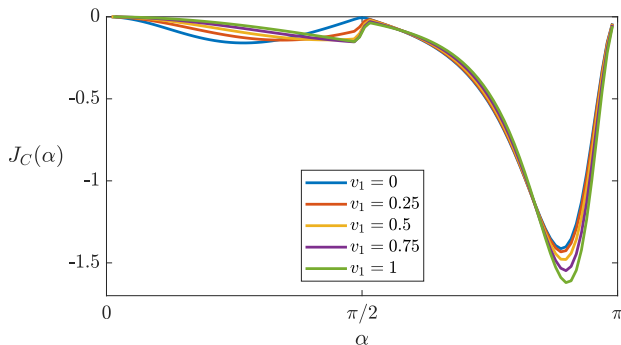


FIG. 3. Current of Chern number pump as a function of the pumping parameter α for different velocity v_1 in the gapped system and $v_0 = 1$ in the lead. Here the system size for the gapped system is chosen as $L = 20$.

dimerized limit, as expected.

D. Current for Chern number pump

As studied in [15, 28, 37], the higher Berry curvature in one dimensional gapped systems characterizes the flow of ordinary Berry curvature as well as the Chern number pump. In this section, to make the Chern-number pump more transparent, we introduce the notion of a current associated with Chern-number transport.

We begin by illustrating the physical picture using the lattice models discussed above. A similar physical picture was used to study the Berry curvature flow in boundary conformal field theories [37]. For the Hamiltonian in Eq. (3.1), one can diagonalize it in the single-particle subspace as

$$H_{\text{gap}} = U^\dagger(\theta, \phi) \begin{pmatrix} H_+(\alpha) & 0 \\ 0 & H_-(\alpha) \end{pmatrix} U(\theta, \phi), \quad (3.22)$$

where (α, θ, ϕ) parametrize the three-dimensional parameter space $X = S^3$ as defined in Eq. (2.7).

If our one-dimensional system possesses a nonzero higher Berry invariant, then each block $H_\pm(\alpha)$ exhibits a $U(1)$ Thouless pump as the parameter α is varied. Notably, $H_+(\alpha)$ and $H_-(\alpha)$ pump $U(1)$ charge in opposite directions, so that the net $U(1)$ charge transport vanishes. However, due to the structure in (3.22), each mode in $H_+(\alpha)$ ($H_-(\alpha)$) carries a quantized Chern number $+1$ (-1) over the two-dimensional parameter subspace $S_{\theta\phi}^2$ spanned by θ and ϕ . Thus, although the $U(1)$ charge pumps cancel, there remains a nontrivial net flow of Berry curvature or Chern number. To characterize this flow, we define the 1-form Chern-number pumping current as

$$J_C(\alpha) = \int_{S_{\theta\phi}^2} \text{Tr}(R^\dagger dR)^{\wedge 3}. \quad (3.23)$$

It is noted that the integral $\int J_C(\alpha)$ is nothing but the higher winding number ν_3 in (1.4).

As shown in Fig. 3, we plot the distribution of $J_C(\alpha)$ for $\alpha \in [0, \pi]$ in the lattice models studied in Sec. III C. For different values of the hopping strength v_1 in (3.16), the detailed profile of $J_C(\alpha)$ changes accordingly. However, its integral, which corresponds to the higher winding number ν_3 , remains invariant, taking the quantized value -1 in all cases considered.

As a remark, the detailed profile of J_C in Fig. 3 also depends on the specific boundary setup. Here the lead is coupled to site $i = 0$ of the gapped system, and one observes that the peak amplitude of J_C appears in the region $\alpha \in [\pi/2, \pi]$. If instead the lead is attached to site $i = 1$, the peak shifts to the region $\alpha \in [0, \pi/2]$. This shift reflects the underlying dimerized structure of the gapped system (See, e.g., Fig. 2). A similar physical picture arises in the study of 3-form higher Berry curvature in lattice systems [15, 28]. Depending on the location at which the Berry-curvature flow is probed, the expression for the higher Berry curvature can vary, even though the associated topological invariant remains unchanged.

E. Robustness against disorder

Now, to further examine the robustness of our topological invariant, we introduce random on-site disorder by adding the following term to the Hamiltonian defined in (3.1) and (3.16):

$$H_{\text{disorder}} = \sum_{i=0}^{2L-1} d_i \psi_i^\dagger \psi_i, \quad (3.24)$$

where $d_i \in \mathbb{R}$ denotes the random on-site potential at site i . The disorder potentials d_i are independently drawn from a uniform distribution on $[0, 2\bar{d}]$, with \bar{d} setting the average disorder strength. As we vary the parameters over the space X , the disorder configuration is kept fixed. This ensures that we are considering a continuous family of Hamiltonians throughout the parameter sweep.

As shown in Fig. 4, for different values of the disorder strength \bar{d} , the detailed profile of the Chern-number current J_C changes accordingly. Nevertheless, its integral, which corresponds to the topological invariant ν_3 , remains quantized at -1 , with deviations within 1% in our numerical calculations³. This demonstrates that the higher winding number defined in Eq. (1.4) is a robust topological invariant.

³ We note that if the disorder strength becomes sufficiently large, the system may undergo a phase transition. In the present analysis, we restrict the disorder strength to a regime where no phase transition occurs within the family of Hamiltonians under consideration.

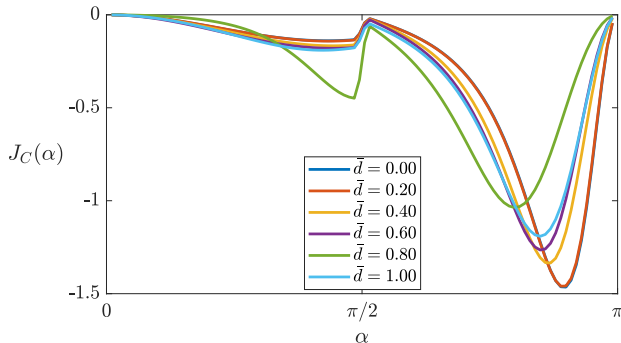


FIG. 4. Current of Chern number pump as a function of the pumping parameter α for different onsite-disorder strengths \bar{d} . We choose $v_0 = 1$, $v_1 = 0.5$, and the gapped-system size is $L = 20$.

IV. DISCUSSION AND CONCLUSION

In this work, we have proposed a boundary scattering approach to detect higher Berry invariants in one dimensional gapped free-fermion systems. We find that the topological information of the gapped system is encoded in the higher winding number of the reflection matrix, which remains robust against perturbations such as disorder.

It is natural to ask whether our formula can be extended to the case where the bulk gapped system is interacting, while the lead remains a free-fermion system⁴. We expect that (1.4) continues to hold in this setting, since in one dimension the higher Berry invariant is a well-defined quantized invariant for all invertible gapped phases [21]. In particular, when interactions are introduced into our gapped free-fermion model, the invariant should remain unchanged as long as the spectral gap stays open throughout the parameter space of the family of systems. It would be interesting to investigate this generalization systematically, for example by adapting the approach in Ref.[69].

Another interesting direction is to extend the boundary-scattering approach to higher-dimensional parametrized gapped systems. For instance, we expect that the formula in (1.4) can be applied to the higher Thouless charge pump in $(2+1)$ dimensions [7]. To realize a $(2+1)d$ higher Thouless pump, two external parameters are required. If the system is defined on a cylinder with translation symmetry along the direction parallel

⁴ If the lead is also interacting, the situation becomes more subtle. In that case, single-particle scattering states may not be well defined, and the notion of a reflection matrix must be replaced by a boundary response formulated in terms of operators of the gapless theory. Different operator sectors can in general experience different boundary phases, so the topological information encoded in the interface may depend on which excitations are used as probes.

to the boundary, the corresponding momentum k can be treated as a third parameter. In this way, (1.4) may be used to detect the higher Thouless pumping invariant through boundary scattering. This perspective also suggests a close connection between the higher Thouless pump in $(2+1)d$ systems and the higher Berry phase in $(1+1)d$ systems, a relation that has indeed been explored in Ref.[21]. It would be interesting to revisit this connection from the viewpoint of boundary physics in future work.

ACKNOWLEDGMENTS

We thank for interesting discussions with Agnes Beaudry, Michael Hermele, Marvin Qi, Shinsei Ryu, Ken Shiozaki, Ophelia Sommer, and Ashvin Vishwanath. This work is supported by a startup at Georgia Institute of Technology.

Appendix A: Details on boundary scattering

1. Reflection matrix through wave function matching

In this appendix we summarize, following Ref. [70], how to extract the reflection matrix from the Green's function. We decompose the total Hamiltonian as

$$H = H_{\text{lead}} + H_{\text{gap}} + H_{\text{int}}, \quad (\text{A1})$$

where H_{lead} describes a semi-infinite lead, H_{gap} the gapped scattering region, and H_{int} their coupling.

We assume a uniform nearest-neighbor hopping lead. Writing the n -component spinor ψ_j^a where $a = 1, \dots, n$ labels the fermion species, the lead Hamiltonian is

$$H_{\text{lead}} = \sum_{j=-\infty}^{-1} \frac{v_0}{2} \left(\psi_{j-1}^\dagger \psi_j + \text{h.c.} \right). \quad (\text{A2})$$

At the interface between $j = -1$ and $j = 0$, we take

$$H_{\text{int}} = \frac{v_0}{2} \left(\psi_{-1}^\dagger \psi_0 + \text{h.c.} \right). \quad (\text{A3})$$

For the scattering region we consider on-site terms and nearest-neighbor hoppings,⁵

$$H_{\text{gap}} = \sum_{j=0}^L \psi_j^\dagger M^j \psi_j + \sum_{j=0}^{L-1} \left(\psi_j^\dagger T^j \psi_{j+1} + \text{h.c.} \right), \quad (\text{A4})$$

⁵ The method extends to general quadratic Hamiltonians; however, the Green's-function construction is typically less transparent and more computationally involved.

where M^j and T^j are $n \times n$ matrices. For simplicity we further assume the hopping is diagonal in species, $T_{ab}^j = t_j \delta_{ab}$.

In the single-particle sector, eigenstates in the lead ($j \leq 0$) are plane waves. Imposing continuity at $j = 0$, we write

$$\psi_j \equiv \langle j | \psi \rangle = \left(e^{ikj} \mathbb{I} + e^{-ikj} R \right) A_0, \quad (j \leq 0), \quad (\text{A5})$$

where R is the $n \times n$ reflection matrix and A_0 is an n -component unit vector specifying the incident channel. Evaluating (A5) at $j = 0$ gives

$$\psi_0 = (\mathbb{I} + R) A_0, \quad (\text{A6})$$

and at $j = -1$ yields

$$\psi_{-1} = (e^{-ik} \mathbb{I} + e^{ik} R) A_0 = e^{ik} \psi_0 - 2i \sin k A_0. \quad (\text{A7})$$

The Schrödinger equation at $j = 0$ reads

$$0 = \langle 0 | (\omega \mathbb{I} - H) | \psi \rangle = (\omega \mathbb{I} - M^0) \psi_0 - \frac{v_0}{2} \psi_{-1} - t_0 \psi_1, \quad (\text{A8})$$

where we used $T^0 = t_0 \mathbb{I}$. Substituting (A7) into (A8) gives

$$\left(\omega \mathbb{I} - M^0 - \Sigma_L \mathbb{I} \right) \psi_0 - t_0 \psi_1 = q_0, \quad (\text{A9})$$

with the (retarded) lead self-energy

$$\Sigma_L = \frac{v_0}{2} e^{ik}, \quad (\text{A10})$$

and the source term

$$q_0 = -iv_0 \sin k A_0. \quad (\text{A11})$$

Therefore the problem reduces to an inhomogeneous equation on the $j \geq 0$ subspace,

$$(\omega \mathbb{I} - H') | \psi \rangle = | q \rangle, \quad (\text{A12})$$

where

$$H'_{ij} = (H_{\text{gap}})_{ij} + \Sigma_L \delta_{i0} \delta_{j0}, \quad q_i = \delta_{i0} q_0, \quad (i, j \geq 0). \quad (\text{A13})$$

Defining the Green's function

$$G(\omega) = (\omega \mathbb{I} - H')^{-1}, \quad (\text{A14})$$

we have $|\psi\rangle = G(\omega) |q\rangle$ and thus

$$\psi_0 = G_{00}(\omega) q_0 = -iv_0 \sin k G_{00}(\omega) A_0, \quad (\text{A15})$$

where $G_{00}(\omega) \equiv \langle 0 | G(\omega) | 0 \rangle$. Combining this with (A6) and using that A_0 is arbitrary, we obtain the reflection matrix

$$R = -\mathbb{I} - iv_0 \sin k G_{00}(\omega). \quad (\text{A16})$$

2. Green's function on lattice

In the previous subsection, we showed that the reflection matrix can be read off directly from the Green's function. In this section we review the continued-fraction method for computing lattice Green's functions.

Working in the single-particle subspace, we partition the Hilbert space as

$$\mathcal{H} = \mathcal{H}_A \oplus \mathcal{H}_B, \quad \mathcal{H}_A = \text{span}\{|0\rangle\}, \quad \mathcal{H}_B = \text{span}\{|i\rangle \mid i \geq 1\}.$$

With respect to this decomposition, the operator $\omega \mathbb{I} - H'$ takes the block form

$$\omega \mathbb{I} - H' = \begin{pmatrix} \omega \mathbb{I} - H'_{AA} & -H'_{AB} \\ -H'_{BA} & \omega \mathbb{I} - H'_{BB} \end{pmatrix}. \quad (\text{A17})$$

Let $G(\omega) = (\omega \mathbb{I} - H')^{-1}$ denote the full Green's function. By the Schur-complement formula,

$$G_{AA}(\omega) = \left[\omega \mathbb{I} - H'_{AA} - H'_{AB} g_B(\omega) H'_{BA} \right]^{-1}, \quad (\text{A18})$$

where we have introduced the Green's function of the decoupled B -subsystem,

$$g_B(\omega) := (\omega \mathbb{I} - H'_{BB})^{-1}.$$

For the 1D chain considered here, the blocks are

$$H'_{AA} = (M^0 + \Sigma_L \mathbb{I}) \otimes |0\rangle \langle 0|, \quad (\text{A19})$$

$$H'_{AB} = t_0 \mathbb{I} \otimes |0\rangle \langle 1|, \quad H'_{BA} = H'_{AB}^\dagger, \quad (\text{A20})$$

$$H'_{BB} = \sum_{j=1}^L M^j \otimes |j\rangle \langle j| + \sum_{j=1}^{L-1} t_j \mathbb{I} \otimes (|j\rangle \langle j+1| + \text{h.c.}). \quad (\text{A21})$$

Since \mathcal{H}_A is one-dimensional in real space, we obtain

$$\begin{aligned} \langle 0 | G(\omega) | 0 \rangle &= \langle 0 | G_{AA}(\omega) | 0 \rangle \\ &= \left[\omega \mathbb{I} - M^0 - \Sigma_L \mathbb{I} - t_0^2 \langle 1 | g_B(\omega) | 1 \rangle \right]^{-1}. \end{aligned} \quad (\text{A22})$$

In other words, $\langle 0 | G(\omega) | 0 \rangle$ is determined by the matrix element $\langle 1 | g_B(\omega) | 1 \rangle$ of the subsystem with site 0 removed.

This observation leads to a recursion. Define $g^{(i)}(\omega)$ as the Green's function of the subsystem restricted to sites $i, i+1, \dots, L$. Then for $1 \leq i \leq L-1$,

$$\langle i | g^{(i)}(\omega) | i \rangle = \left[\omega \mathbb{I} - M^i - t_i^2 \langle i+1 | g^{(i+1)}(\omega) | i+1 \rangle \right]^{-1}, \quad (\text{A23})$$

with terminal condition (open boundary at L)

$$\langle L | g^{(L)}(\omega) | L \rangle = (\omega \mathbb{I} - M^L)^{-1}. \quad (\text{A24})$$

Substituting these expressions back inductively yields $\langle 1 | g_B(\omega) | 1 \rangle$, and hence $\langle 0 | G(\omega) | 0 \rangle$ via Eq. (A22).

While this continued-fraction evaluation is straightforward numerically, it typically does not yield a compact closed form. A major simplification occurs when the sample is translationally invariant (e.g., $M^i = M$ and $t_i = t$ in the bulk), in which case the recursion reduces to a self-consistency equation for the surface Green's function.

Appendix B: Detecting Thouless charge pump via boundary scattering

In this appendix, we apply the boundary-scattering approach to detect the topological invariant associated with the Thouless $U(1)$ charge pump, where the parameter space is $X = S^1$. The model and method we consider are closely related to those studied in Ref.[57]. This example serves as a useful illustration for understanding the detection of higher Berry phases discussed in the main text.

We model the (semi-infinite) lead as a free-fermion tight-binding chain with nearest-neighbor hopping,

$$H_{\text{lead}} = \sum_{i=-\infty}^{-1} \frac{v_0}{2} (\psi_{i+1}^\dagger \psi_i + \text{h.c.}). \quad (\text{B1})$$

For an infinite chain (or away from the boundary), Fourier transforming $\psi_i = \int \frac{dk}{2\pi} e^{ik_i} \psi_k$ gives

$$H_{\text{lead}} = \int_{-\pi}^{\pi} \frac{dk}{2\pi} \varepsilon(k) \psi_k^\dagger \psi_k, \quad \varepsilon(k) = v_0 \cos k. \quad (\text{B2})$$

Thus the zero-energy (Fermi) points satisfy $\varepsilon(k_F) = 0$, i.e., $k_F = \pm \frac{\pi}{2}$. The group velocity is

$$v(k) = \frac{\partial \varepsilon(k)}{\partial k} = -v_0 \sin k, \quad (\text{B3})$$

so the Fermi velocity has magnitude $|v_F| = v_0$ at $k_F = \pm \frac{\pi}{2}$ (with the sign distinguishing left-/right-movers).

1. $U(1)$ Thouless pump and boundary scattering

A Thouless pump can be realized in a one-dimensional free-fermion system whose (generally complex) mass terms are controlled by an external parameter $\alpha : [0, T] \rightarrow S^1$. When $\alpha(t)$ is varied adiabatically through one full cycle, an integer number of charges is transported across the system. In a translation-invariant geometry this transport is captured by the change of bulk polarization over the cycle. Equivalently, the total charge pumped per period is the first Chern number obtained by integrating the Berry curvature over the two-torus formed by the Brillouin zone and the pump parameter space S^1 .

If the system is opened, the same topological invariant appears as spectral flow of edge states: during one adiabatic cycle, an edge level traverses the gap so that one electron is transferred from the right boundary to the left boundary. The same physics is visible in a scattering setup where metallic leads are attached to one end of the pump. In the insulating limit the lead electron is perfectly reflected, acquiring a parameter-dependent phase,

$$\psi_{\text{out}}^{\text{lead}}(t) = R(\alpha(t)) \psi_{\text{in}}^{\text{lead}}(t), \quad (\text{B4})$$

with $R(\alpha(t)) = e^{i\beta(t)}$. The accumulated phase then produces a pumped charge given by Brouwer's formula [71],

$$\begin{aligned} \Delta Q &= \frac{e}{2\pi} \int_0^T dt R^\dagger \partial_t R = \frac{e}{2\pi} \int_0^T dt \partial_t \beta(t) \\ &= \frac{e}{2\pi} [\beta(T) - \beta(0)]. \end{aligned} \quad (\text{B5})$$

While the detailed time dependence of $\alpha(t)$ and $\beta(t)$ may differ, over a closed cycle they have the same net winding. Consequently, the pumped charge per period is quantized and equals the common winding number [72, 73].

2. Thouless charge pump in the decoupled limit

Before tackling the full sample Hamiltonian, it is useful to start with a simpler decoupled limit, in which the sample is described by

$$\begin{aligned} H_{\text{dimer}} &= \sum_{i=0}^L (-1)^i m_1 a_i^\dagger \psi_i + \sum_{i=0}^L f_+(m_0) (\psi_{2i+1}^\dagger \psi_{2i} + \text{h.c.}) \\ &\quad + \sum_{i=1}^L f_-(m_0) (\psi_{2i-1}^\dagger \psi_i + \text{h.c.}), \end{aligned} \quad (\text{B6})$$

where

$$f_+(m_0) = \begin{cases} m_0, & m_0 \geq 0, \\ 0, & \text{otherwise,} \end{cases} \quad (\text{B7})$$

and

$$f_-(m_0) = \begin{cases} -m_0, & m_0 \leq 0, \\ 0, & \text{otherwise.} \end{cases} \quad (\text{B8})$$

We consider the parameter space $X = S^1$ by restricting to the loop $m_0^2 + m_1^2 = m^2$ at fixed m .

Because H_{dimer} is decoupled, the Green's function element G_{00} depends only on the degrees of freedom directly coupled to site 0. Thus, for the purpose of computing G_{00} , we may replace the full system by the effective local Hamiltonian

$$H_{\text{eff}} = \begin{cases} m_1 (\psi_0^\dagger \psi_0 - \psi_1^\dagger \psi_1) + m_0 (\psi_0^\dagger \psi_1 + \psi_1^\dagger \psi_0), & m_0 > 0, \\ m_1 \psi_0^\dagger \psi_0, & m_0 \leq 0. \end{cases} \quad (\text{B9})$$

This decoupled system is effectively of finite size, so G_{00} can be obtained directly. In the following we focus on fermions near the Fermi surface, $\omega = 0$ and $k = \pi/2$.

For $m_0 > 0$, one finds

$$G_{00} = \left(-m_1 - \frac{iv_0}{2} + \frac{m_0^2}{m_1} \right)^{-1} = \frac{-2m_1}{2m^2 + iv_0 m_1}, \quad (\text{B10})$$

where $m^2 = m_0^2 + m_1^2$. Using (3.6), the reflection amplitude is

$$R = -\frac{2m^2 - iv_0 m_1}{2m^2 + iv_0 m_1}. \quad (\text{B11})$$

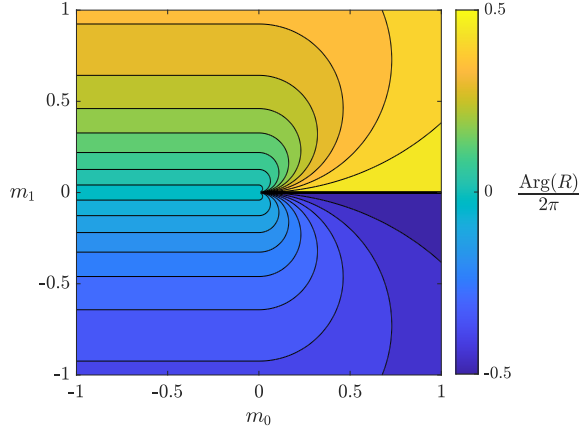


FIG. 5. $\frac{1}{2\pi} \text{Arg}(R)$ for different values of m_0 and m_1 in the decoupled limit, with lead velocity $v_0 = 1$.

For $m_0 \leq 0$, we instead have

$$G_{00} = \left(-m_1 - \frac{iv_0}{2} \right)^{-1} = \frac{-2}{2m_1 + iv_0}, \quad (\text{B12})$$

and therefore

$$R = -\frac{2m_1 - iv_0}{2m_1 + iv_0}. \quad (\text{B13})$$

Since $|R| = 1$, the contour integral over a loop C enclosing the origin. $\oint_C R^{-1} dR$ reduces to the net winding of $\text{Arg}(R)$ along C . This integer winding equals the number of charges pumped across the system during one cycle of the parameter variation. As shown in Fig.5, the reflection phase winds by a full 2π for any loop that circles the origin once.

To make this explicit, we parametrize the loop as $(m_0, m_1) = (\cos \alpha, \sin \alpha)$. The reflection phase then generates a pumped current [71]

$$J(\alpha) = \frac{1}{2\pi} R^\dagger(\alpha) \partial_\alpha R(\alpha), \quad (\text{B14})$$

where we set the electron charge to $e = 1$. This gives

$$J(\alpha) = \begin{cases} \frac{4 \cos \alpha}{(-9 + \cos 2\alpha)\pi}, & m_0 > 0, \\ \frac{2 \cos \alpha}{(1 + 4 \sin^2 \alpha)\pi}, & m_0 \leq 0. \end{cases} \quad (\text{B15})$$

As shown in Fig. 6, we give a plot of $J(\alpha)$ as a function of $\alpha \in [0, \pi]$ according to the above equation. Integrating over one full cycle gives an exactly quantized result,

$$\Delta Q = \int_0^{2\pi} J(\alpha) d\alpha = -1, \quad (\text{B16})$$

indicating that one unit of charge is pumped per loop in parameter space.

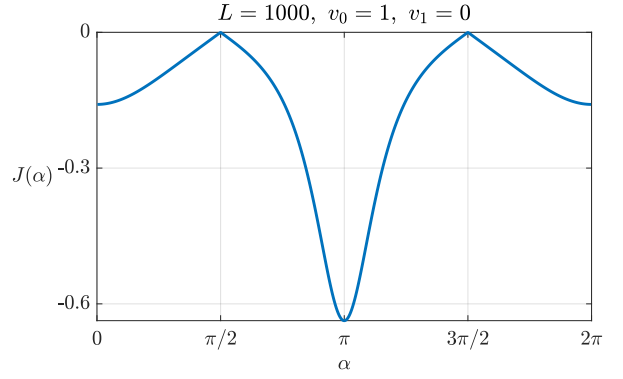


FIG. 6. $J(\alpha)$ as a function of α in the decoupled limit, plotted according to (B15).

3. Charge pump with hoppings

Next, we turn on the group velocity v_1 within the sample by adding uniform hopping terms to Eq. (B6)

$$H_{\text{gap}} = H_{\text{dimer}} + \sum_{i=0}^{2L-1} \frac{v_1}{2} (\psi_{i+1}^\dagger \psi_i + \text{h.c.}) \quad (\text{B17})$$

Again, we consider the low energy fermions with $\omega = 0$ and $k = \frac{\pi}{2}$.

For $m_0 > 0$

$$G_{00}^{(0)} = \left(-m_1 - \frac{iv_0}{2} - \left(\frac{v_1}{2} + m_0 \right)^2 G_{11}^{(1)} \right)^{-1}, \quad (\text{B18})$$

$$G_{11}^{(1)} = \left(m_1 - \frac{v_1^2}{4} G_{22}^{(2)} \right)^{-1}, \quad (\text{B19})$$

$$G_{22}^{(2)} = \left(-m_1 - \left(\frac{v_1}{2} + m_0 \right)^2 G_{33}^{(3)} \right)^{-1}. \quad (\text{B20})$$

Since our Hamiltonian has translational symmetry with unit cell of 2 sites, in the $L \rightarrow \infty$ limit we have $G_{11}^{(1)} = G_{33}^{(3)}$. Solving for the quadratic equation, we get

$$G_{11}^{(1)} = \frac{2 \left(m_0^2 - m_1^2 + m_0 v_1 + m \sqrt{m_1^2 + (m_0 + v_1)^2} \right)}{(v_1 + 2m_0)^2 m_1}, \quad (\text{B21})$$

where $m = \sqrt{m_0^2 + m_1^2}$, and we choose the solution that has a smooth limit at $v_1 = 0$. In order to match the result in the decoupled limit $v_1 = 0$, we choose the + solution. Therefore,

$$G_{00}^{(0)} = \frac{2m_1}{m^2 + m_0 v_1 - m \sqrt{m_1^2 + (m_0 + v_1)^2} + im_1 v_0}. \quad (\text{B22})$$

The reflection coefficient is given by

$$R = -\frac{m^2 + m_0 v_1 + m \sqrt{m_1^2 + (m_0 + v_1)^2} - im_1 v_0}{m^2 + m_0 v_1 + m \sqrt{m_1^2 + (m_0 + v_1)^2} + im_1 v_0}. \quad (\text{B23})$$

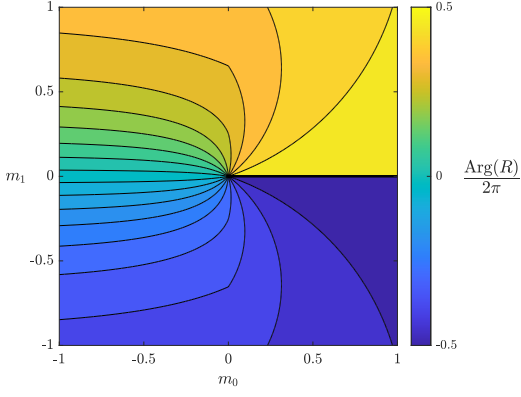


FIG. 7. $\frac{1}{2\pi}\text{Arg}(R)$ for different values of m_0 and m_1 in the case where $v_0 = v_1 = 1$.

For $m_0 < 0$, we have instead

$$G_{00}^{(0)} = \left(-m_1 - \frac{iv_0}{2} - \frac{v_1^2}{4} G_{11}^{(1)} \right)^{-1}, \quad (\text{B24})$$

$$G_{11}^{(1)} = \left(m_1 - \left(\frac{v_1}{2} - m_0 \right)^2 G_{22}^{(2)} \right)^{-1}, \quad (\text{B25})$$

$$G_{22}^{(2)} = \left(-m_1 - \frac{v_1^2}{4} G_{33}^{(3)} \right)^{-1}. \quad (\text{B26})$$

Again, in the $L \rightarrow \infty$ limit we have $G_{11}^{(1)} = G_{33}^{(3)}$, which leads to

$$G_{11}^{(1)} = \frac{2 \left(-m_0^2 - m_1^2 + m_0 v_1 + m \sqrt{m_1^2 + (m_0 + v_1)^2} \right)}{v_1^2 m_1}, \quad (\text{B27})$$

where we select the branch of the solution that remains smooth in the limit $v_1 \rightarrow 0$. Therefore,

$$G_{00}^{(0)} = \frac{2m_1}{m_0^2 - m_1^2 + m_0 v_1 + m \sqrt{m_1^2 + (m_0 + v_1)^2} - im_1 v_0}. \quad (\text{B28})$$

The reflection coefficient is given by

$$R = - \frac{-m_0^2 + m_1^2 + m_0 v_1 + m \sqrt{m_1^2 + (m_0 - v_1)^2} - im_1 v_0}{-m_0^2 + m_1^2 + m_0 v_1 + m \sqrt{m_1^2 + (m_0 - v_1)^2} + im_1 v_0}. \quad (\text{B29})$$

As shown in Fig. 7, the phase of reflection $\text{Arg}(R)$ will undergo a full 2π winding along any loop C enclosing the origin, i.e., $\int_C R^{-1} dR = 2\pi$.

4. Charge pump with hoppings and disorders

In order to verify that the effect is topologically robust, we add onsite disorder to the sample Hamiltonian,

$$H_{\text{disorder}} = \sum_{j=0}^{\infty} d_j \psi_j^\dagger \psi_j, \quad (\text{B30})$$

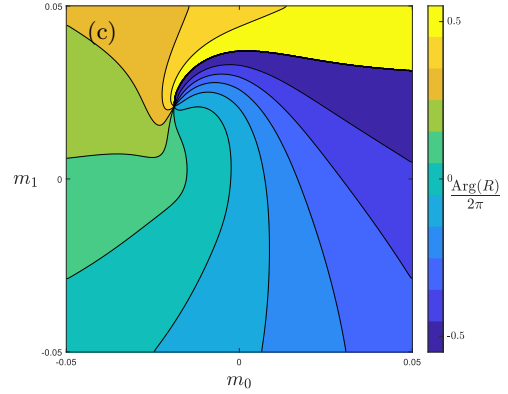
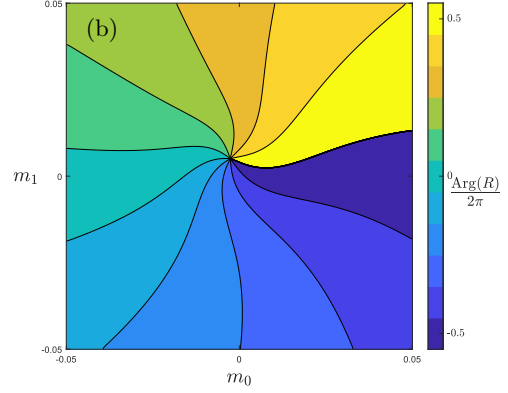
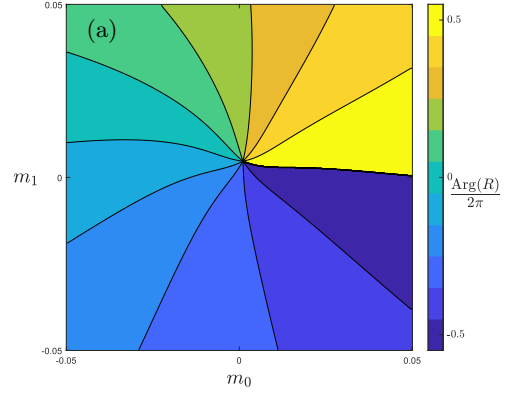


FIG. 8. The phases $\text{Arg}(R)$ for disorder strength (a) $\bar{d} = 0.05$, (b) $\bar{d} = 0.10$, (c) $\bar{d} = 0.15$ with a system size $L = 100$, $v_0 = 1$, $v_1 = 1$. Notice that we show the zoomed-in view near the origin to better visualize the distortion due to the disorder.

where d_j are random onsite potentials with mean strength \bar{d} , drawn from a uniform distribution on $[0, 2\bar{d}]$.

We take a system size $L = 100$ and solve for the wave function numerically. As shown in Fig. 8, the presence of disorder slightly shifts the locations of the sinks and distorts the phase diagram. Nevertheless, the topological signature remains unchanged: $\text{Arg}(R)$ winds by 2π along any sufficiently large closed loop that encloses a sink, demonstrating robustness against this class of disorder.

As a final remark, in Figs. 5, 7, and 8, one can clearly observe singularities in $\text{Arg}(R)$. These singularities cor-

respond to gapless points in the phase diagram, whose general properties have been the subject of extensive recent study.

-
- [1] A. Kitaev, Toward a topological classification of many-body quantum states with short-range entanglement (2011), talk at Simons Center for Geometry and Physics <http://scgp.stonybrook.edu/archives/1087>.
- [2] A. Kitaev, On the classification of short-range entangled states (2013), talk at Simons Center for Geometry and Physics <http://scgp.stonybrook.edu/archives/16180>.
- [3] A. Kitaev, Homotopy-theoretic approach to SPT phases in action: \mathbb{Z}_{16} -classification of three-dimensional superconductors (2015), talk at workshop *Symmetry and Topology in Quantum Matter*, Institute for Pure & Applied Mathematics, University of California Los Angeles.
- [4] A. Kitaev, Differential forms on the space of statistical mechanics models (2019), talk at the conference in celebration of Dan Freed's 60th birthday: <https://web.ma.utexas.edu/topqft/talkslides/kitaev.pdf>.
- [5] J. C. Y. Teo and C. L. Kane, Topological defects and gapless modes in insulators and superconductors, *Phys. Rev. B* **82**, 115120 (2010).
- [6] A. Kapustin and L. Spodyneiko, Higher-dimensional generalizations of berry curvature, *Physical Review B* **101**, 10.1103/physrevb.101.235130 (2020).
- [7] A. Kapustin and L. Spodyneiko, Higher-dimensional generalizations of the Thouless charge pump (2020), [arXiv:2003.09519](https://arxiv.org/abs/2003.09519) [cond-mat.str-el].
- [8] A. Kapustin and N. Sopenko, Local Noether theorem for quantum lattice systems and topological invariants of gapped states, *Journal of Mathematical Physics* **63**, 091903 (2022), [arXiv:2201.01327](https://arxiv.org/abs/2201.01327) [math-ph].
- [9] P.-S. Hsin, A. Kapustin, and R. Thorngren, Berry phase in quantum field theory: Diabolical points and boundary phenomena, *Phys. Rev. B* **102**, 245113 (2020), [arXiv:2004.10758](https://arxiv.org/abs/2004.10758) [cond-mat.str-el].
- [10] C. Cordova, D. Freed, H. T. Lam, and N. Seiberg, Anomalies in the space of coupling constants and their dynamical applications I, *SciPost Physics* **8**, 10.21468/scipostphys.8.1.001 (2020).
- [11] C. Cordova, D. Freed, H. T. Lam, and N. Seiberg, Anomalies in the space of coupling constants and their dynamical applications II, *SciPost Physics* **8**, 10.21468/scipostphys.8.1.002 (2020).
- [12] D. V. Else, Topological goldstone phases of matter, *Physical Review B* **104**, 10.1103/physrevb.104.115129 (2021).
- [13] S. Bachmann, W. De Roeck, M. Fraas, and T. Jappens, A classification of G -charge Thouless pumps in 1D invertible states, [arXiv e-prints](https://arxiv.org/abs/2204.03763), [arXiv:2204.03763](https://arxiv.org/abs/2204.03763) (2022), [arXiv:2204.03763](https://arxiv.org/abs/2204.03763) [math-ph].
- [14] Y. Choi and K. Ohmori, Higher berry phase of fermions and index theorem, *Journal of High Energy Physics* **2022**, 10.1007/jhep09(2022)022 (2022).
- [15] X. Wen, M. Qi, A. Beaudry, J. Moreno, M. J. Pflaum, D. Spiegel, A. Vishwanath, and M. Hermele, Flow of higher Berry curvature and bulk-boundary correspondence in parametrized quantum systems, *Phys. Rev. B* **108**, 125147 (2023), [arXiv:2112.07748](https://arxiv.org/abs/2112.07748) [cond-mat.str-el].
- [16] D. Aasen, Z. Wang, and M. B. Hastings, Adiabatic paths of hamiltonians, symmetries of topological order, and automorphism codes, *Physical Review B* **106**, 10.1103/physrevb.106.085122 (2022).
- [17] P.-S. Hsin and Z. Wang, On topology of the moduli space of gapped hamiltonians for topological phases, *Journal of Mathematical Physics* **64**, 041901 (2023).
- [18] K. Shiozaki, Adiabatic cycles of quantum spin systems, *Physical Review B* **106**, 10.1103/physrevb.106.125108 (2022).
- [19] S. Ohyama, K. Shiozaki, and M. Sato, Generalized Thouless pumps in $(1+1)$ -dimensional interacting fermionic systems, *Phys. Rev. B* **106**, 165115 (2022).
- [20] S. Ohyama, Y. Terashima, and K. Shiozaki, Discrete higher berry phases and matrix product states (2023), [arXiv:2303.04252](https://arxiv.org/abs/2303.04252) [cond-mat.str-el].
- [21] A. Artymowicz, A. Kapustin, and N. Sopenko, Quantization of the higher Berry curvature and the higher Thouless pump, [arXiv e-prints](https://arxiv.org/abs/2305.06399), [arXiv:2305.06399](https://arxiv.org/abs/2305.06399) (2023), [arXiv:2305.06399](https://arxiv.org/abs/2305.06399) [math-ph].
- [22] A. Beaudry, M. Hermele, J. Moreno, M. Pflaum, M. Qi, and D. Spiegel, Homotopical foundations of parametrized quantum spin systems (2023), [arXiv:2303.07431](https://arxiv.org/abs/2303.07431) [math-ph].
- [23] S. Ohyama and S. Ryu, Higher structures in matrix product states, [arXiv e-prints](https://arxiv.org/abs/2304.05356), [arXiv:2304.05356](https://arxiv.org/abs/2304.05356) (2023), [arXiv:2304.05356](https://arxiv.org/abs/2304.05356) [cond-mat.str-el].
- [24] M. Qi, D. T. Stephen, X. Wen, D. Spiegel, M. J. Pflaum, A. Beaudry, and M. Hermele, Charting the space of ground states with tensor networks, *SciPost Phys.* **18**, 168 (2025).
- [25] K. Shiozaki, N. Heinsdorf, and S. Ohyama, Higher Berry curvature from matrix product states, [arXiv e-prints](https://arxiv.org/abs/2305.08109), [arXiv:2305.08109](https://arxiv.org/abs/2305.08109) (2023), [arXiv:2305.08109](https://arxiv.org/abs/2305.08109) [quant-ph].
- [26] L. Spodyneiko, Hall conductivity pump, [arXiv e-prints](https://arxiv.org/abs/2309.14332), [arXiv:2309.14332](https://arxiv.org/abs/2309.14332) (2023), [arXiv:2309.14332](https://arxiv.org/abs/2309.14332) [cond-mat.mes-hall].
- [27] A. Debray, S. K. Devalapurkar, C. Krulewski, Y. L. Liu, N. Pacheco-Tallaj, and R. Thorngren, A Long Exact Sequence in Symmetry Breaking: order parameter constraints, defect anomaly-matching, and higher Berry phases, [arXiv e-prints](https://arxiv.org/abs/2309.16749), [arXiv:2309.16749](https://arxiv.org/abs/2309.16749) (2023), [arXiv:2309.16749](https://arxiv.org/abs/2309.16749) [hep-th].
- [28] O. E. Sommer, X. Wen, and A. Vishwanath, Higher Berry Curvature from the Wave Function. I. Schmidt Decomposition and Matrix Product States, *Phys. Rev. Lett.* **134**, 146601 (2025), [arXiv:2405.05316](https://arxiv.org/abs/2405.05316) [cond-mat.str-el].
- [29] O. E. Sommer, A. Vishwanath, and X. Wen, Higher Berry curvature from the wave function. II. Locally parametrized states beyond one dimension, *Phys. Rev. B* **111**, 155110 (2025), [arXiv:2405.05323](https://arxiv.org/abs/2405.05323) [cond-mat.str-el].
- [30] S. Ohyama and S. Ryu, Higher Berry connection for matrix product states, *Phys. Rev. B* **111**, 035121 (2025), [arXiv:2405.05327](https://arxiv.org/abs/2405.05327) [cond-mat.str-el].
- [31] S. Ohyama and S. Ryu, Higher Berry phase from pro-

- jected entangled pair states in (2+1) dimensions, *Phys. Rev. B* **111**, 045112 (2025), [arXiv:2405.05325 \[cond-mat.str-el\]](#).
- [32] B. Liu, J. Zhang, S. Ohyama, Y. Kusuki, and S. Ryu, Multi wavefunction overlap and multi entropy for topological ground states in (2+1) dimensions, *arXiv e-prints*, [arXiv:2410.08284](#) (2024), [arXiv:2410.08284 \[cond-mat.str-el\]](#).
- [33] R. Geiko, Parameterized topological phases in 1d and T-duality, *arXiv e-prints*, [arXiv:2412.20905](#) (2024), [arXiv:2412.20905 \[math-ph\]](#).
- [34] A. Beaudry, M. Hermele, M. J. Pflaum, M. Qi, D. D. Spiegel, and D. T. Stephen, A classifying space for phases of matrix product states (2025), [arXiv:2501.14241 \[math-ph\]](#).
- [35] A. Kapustin, Topological phases of matter and homotopy theory, in *Encyclopedia of Mathematical Physics (Second Edition)*, edited by R. Szabo and M. Bojowald (Academic Press, Oxford, 2025) second edition ed., pp. 106–110.
- [36] Y. Choi, H. Ha, D. Kim, Y. Kusuki, S. Ohyama, and S. Ryu, Higher structures on boundary conformal manifolds: Higher berry phase and boundary conformal field theory (2025), [arXiv:2507.12525 \[hep-th\]](#).
- [37] X. Wen, Space of conformal boundary conditions from the view of higher berry phase: Flow of berry curvature in parametrized bcfts (2025), [arXiv:2507.12546 \[hep-th\]](#).
- [38] A. Prakash, M. Fava, and S. A. Parameswaran, Universality and Unnecessary Criticality in One Dimension, *Phys. Rev. Lett.* **130**, 256401 (2023), [arXiv:2209.00037 \[cond-mat.str-el\]](#).
- [39] A. Prakash and S. A. Parameswaran, Charge pumps, boundary modes, and the necessity of unnecessary criticality, *Phys. Rev. B* **112**, L241117 (2025), [arXiv:2408.15351 \[cond-mat.str-el\]](#).
- [40] N. Manjunath and D. V. Else, Anomalous continuous symmetries and quantum topology of goldstone modes, *Physical Review B* **111**, 10.1103/physrevb.111.125151 (2025).
- [41] A. Bose, A. Hardy, N. Manjunath, and A. Paramekanti, Symmetry constrained field theories for chiral spin liquid to spin crystal transitions (2025), [arXiv:2505.01491 \[cond-mat.str-el\]](#).
- [42] N. G. Jones, R. Thorngren, R. Verresen, and A. Prakash, Charge pumps, pivot hamiltonians and symmetry-protected topological phases (2025), [arXiv:2507.00995 \[cond-mat.str-el\]](#).
- [43] Y. Kubota, Stable homotopy theory of invertible gapped quantum spin systems i: Kitaev's ω -spectrum (2025), [arXiv:2503.12618 \[math-ph\]](#).
- [44] Y. Choi, Higher connection in open string field theory (2026), [arXiv:2602.13627 \[hep-th\]](#).
- [45] T. D. Brennan and K. Intriligator, Generalized families of qfts (2026), [arXiv:2602.09105 \[hep-th\]](#).
- [46] C. Copetti, 't hooft anomalies and defect conformal manifolds: Topological signatures from modulated effective actions (2025), [arXiv:2507.15466 \[hep-th\]](#).
- [47] K. Shiozaki, Equivariant parameter families of spin chains: A discrete mps formulation (2025), [arXiv:2507.19932 \[quant-ph\]](#).
- [48] N. Manjunath and D. V. Else, In search of diabolical critical points, *arXiv e-prints*, [arXiv:2601.10783](#) (2026), [arXiv:2601.10783 \[cond-mat.str-el\]](#).
- [49] K. Inamura and S. Ohyama, Generalized cluster states in 2+1d: non-invertible symmetries, interfaces, and parameterized families, *arXiv e-prints*, [arXiv:2601.08615](#) (2026), [arXiv:2601.08615 \[cond-mat.str-el\]](#).
- [50] S. Ohyama and K. Inamura, Parameterized families of 2+1d G -cluster states, *arXiv e-prints*, [arXiv:2601.08616](#) (2026), [arXiv:2601.08616 \[cond-mat.str-el\]](#).
- [51] Y. Li, M. Dell'acqua, and A. Mitra, Classification of Thouless pumps with non-invertible symmetries and implications for Floquet phases, *arXiv e-prints*, [arXiv:2510.01626](#) (2025), [arXiv:2510.01626 \[cond-mat.str-el\]](#).
- [52] Y. Ji, Y. Chung, D. Sprinzak, M. Heiblum, D. Mahalu, and H. Shtrikman, An electronic mach-zehnder interferometer, *Nature* **422**, 415 (2003).
- [53] D. J. Thouless, Quantization of particle transport, *Phys. Rev. B* **27**, 6083 (1983).
- [54] M. Büttiker, H. Thomas, and A. Prêtre, Current partition in multiprobe conductors in the presence of slowly oscillating external potentials, *Zeitschrift für Physik B Condensed Matter* **94**, 133 (1994).
- [55] P. W. Brouwer, Scattering approach to parametric pumping, *Phys. Rev. B* **58**, R10135 (1998), [arXiv:cond-mat/9808347 \[cond-mat.mes-hall\]](#).
- [56] J. E. Avron, A. Elgart, G. M. Graf, and L. Sadun, Transport and Dissipation in Quantum Pumps, *Journal of Statistical Physics* **116**, 425 (2004), [arXiv:math-ph/0305049 \[math-ph\]](#).
- [57] C.-H. Chern, S. Onoda, S. Murakami, and N. Nagaosa, Quantum charge pumping and electric polarization in anderson insulators, *Phys. Rev. B* **76**, 035334 (2007).
- [58] G. Bräunlich, G. M. Graf, and G. Ortelli, Equivalence of Topological and Scattering Approaches to Quantum Pumping, *Communications in Mathematical Physics* **295**, 243 (2010), [arXiv:0902.4638 \[math-ph\]](#).
- [59] N. Doll, H. Schulz-Baldes, and N. Waterstraat, *Spectral flow: A functional analytic and index-theoretic approach* (De Gruyter, 2023).
- [60] K. Shiozaki, A discrete formulation for three-dimensional winding number, *arXiv e-prints*, [arXiv:2403.05291](#) (2024), [arXiv:2403.05291 \[cond-mat.mes-hall\]](#).
- [61] E. Prodan and H. Schulz-Baldes, Bulk and boundary invariants for complex topological insulators, *K* (2016).
- [62] A. R. Akhmerov, J. P. Dahlhaus, F. Hassler, M. Wimmer, and C. W. J. Beenakker, Quantized Conductance at the Majorana Phase Transition in a Disordered Superconducting Wire, *Phys. Rev. Lett.* **106**, 057001 (2011), [arXiv:1009.5542 \[cond-mat.mes-hall\]](#).
- [63] A. R. Akhmerov, J. P. Dahlhaus, F. Hassler, M. Wimmer, and C. W. J. Beenakker, Quantized conductance at the majorana phase transition in a disordered superconducting wire, *Phys. Rev. Lett.* **106**, 057001 (2011).
- [64] M. Wimmer, A. R. Akhmerov, J. P. Dahlhaus, and C. W. J. Beenakker, Quantum point contact as a probe of a topological superconductor, *New Journal of Physics* **13**, 053016 (2011).
- [65] I. C. Fulga, F. Hassler, and A. R. Akhmerov, Scattering theory of topological insulators and superconductors, *Physical Review B* **85**, 10.1103/physrevb.85.165409 (2012).
- [66] G. Y. Cho, K. Shiozaki, S. Ryu, and A. W. W. Ludwig, Relationship between symmetry protected topological phases and boundary conformal field theories via the entanglement spectrum, *Journal of Physics A Mathematical General* **50**, 304002 (2017), [arXiv:1606.06402 \[cond-mat.str-el\]](#).

- [67] H. Schulz-Baldes and D. Toniolo, Dimensional reduction and scattering formulation for even topological invariants, *Communications in Mathematical Physics* **381**, [10.1007/s00220-020-03886-y](https://doi.org/10.1007/s00220-020-03886-y) (2020).
- [68] A. M. Essin and V. Gurarie, Bulk-boundary correspondence of topological insulators from their respective green's functions, *Phys. Rev. B* **84**, 125132 (2011).
- [69] J. E. Avron, A. Elgart, G. M. Graf, L. Sadun, and K. Schnee, *Adiabatic charge pumping in open quantum systems* (2003), [arXiv:math-ph/0209029](https://arxiv.org/abs/math-ph/0209029) [math-ph].
- [70] V. M. K. G. Brocks, P. A. K. P. J. Kelly, I. Marushchenko, T. N. A. Starikov, M. Talanana (Twente), C. R. I. Turek (Brno), C. K. Xia (Beijing), T. N. P. X. Xu (Twente), P. M. Zwierzycki (Poznan), and G. E., Calculating scattering matrices by wave function matching, *Psi-K network* (2007).
- [71] P. W. Brouwer, Scattering approach to parametric pumping, *Physical Review B* **58**, [10.1103/physrevb.58.r10135](https://doi.org/10.1103/physrevb.58.r10135) (1998).
- [72] G. Bräunlich, G. M. Graf, and G. Ortelli, Equivalence of topological and scattering approaches to quantum pumping, *Communications in Mathematical Physics* **295**, [10.1007/s00220-009-0983-1](https://doi.org/10.1007/s00220-009-0983-1) (2009).
- [73] I. C. Fulga, F. Hassler, A. R. Akhmerov, and C. W. J. Beenakker, Scattering formula for the topological quantum number of a disordered multimode wire, *Phys. Rev. B* **83**, 155429 (2011).